Computer-Aided Design of Microstrip Filters Considering Dispersion, Loss, and Discontinuity Effects

REZA MEHRAN

Abstract—**A computer-aided design procedure of microstrip filters involving junctions and discontinuities is investigated.**

The analysis of microstrip filters is described in detail considering dispersion, loss, and the frequency dependent properties of the microstrip discontinuities. It is found that the described analysis procedure leads to an accurate and fast numerical computation of the microstrip filter properties. The theoretical results for some filter structures are compared with measurements, and theory and experiment are found to correspond closely.

I. Introduction

IN A MANNER analogous to the design of classical *LC*-filters involving lumped elements, a variety of microwave filters can be realized in microstrip technique [1]–[3]. These filters often consist of a cascade connection of line sections, steps, T-junctions, and crossings with one or two open-circuited, short-circuited, as well as mismatched far ends. In this approach it is assumed that a short length of high- or low-impedance line terminated at both ends by a low- or high-impedance line has an effect equivalent to that of a series inductance or shunt capacitance, respectively. A lumped series- or parallel-resonant shunt element can be approximated by means of a T-junction or crossing, open- or short-circuited at their far ends, respectively. These resonant elements can be realized also in the manner shown in Fig. 2(d) and (e). In this case the far ends of the discontinuities are loaded with a distributed capacitive element (*C*-element).

In the conversion of the lumped *LC*-elements into the distributed *LC*-elements, the discontinuity and junction effects are considered according to [9]–[11]. This brings about an improved description of the computed transmission properties at high frequencies. Consequently, in designing filters, fewer experiments will be needed to get a proposed transmission characteristic.

The intention of this paper is to introduce a computer-aided design procedure for the fabrication of microstrip filters which contains the filter elements illustrated in Fig. 2 or related filter elements considering the discontinuities shown in Fig. 1. By this means, an accurate and fast numerical analysis or synthesis can be achieved, and in many cases time-consuming "cut-and-try-techniques" may be eliminated from design.

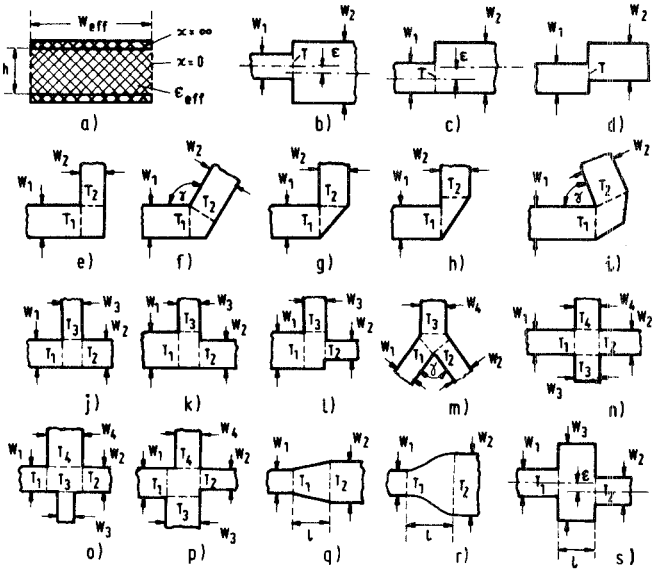

Fig. 1. Microstrip discontinuities.

The design procedure investigated in this work consists of the following steps.

1) On the basis of a tolerance scheme and with the class of the filter specified (e.g., Chebyshev, Butterworth, Cauer, etc.), the *LC*-circuit with lumped elements is determined according to the above mentioned conventional synthesis methods.

2) With the *LC*-element values known, the conversion into the distributed line elements is carried out.This provides an initial configuration for the subsequent computer-aided design steps.

3) Computer optimization is employed to modify the geometrical dimensions of the distributed filter structure in such a way that optimal electrical performance is obtained. Hence, discontinuity effects are included in the analysis.

The determination of the approximate transmission

Manuscript received July 6, 1978; revised October 6, 1978.

The author is with the Lehrstuhl für Allgemeine und Theoretische Elektrotechnik, Department of Electrical Engineering, University of Duisburg, Duisburg, Germany.

0018-9480/79/0300-0239$00.75 ©1979 IEEE

characteristic of a selected filter as a low-pass, bandpass, band-stop, or high-pass filter and the computation of its corresponding lumped element LC-circuit as well as the subsequent conversion into a microstrip line structure are based on theories well known in the literature [1]–[3]. However, the analysis of the filter structure presented in this paper is based on consideration of the frequency-dependent properties of the involved microstrip discontinuities. The optimization of the filters cannot be achieved only by changing of the filter structure dimensions, but also by the application of unsymmetrical discontinuities. The latter ones provide more possibility in optimization procedure. To ensure that the filter structure can be placed into a given area of the substrate within a fixed microwave circuit, discontinuities like bends and Y-junctions can be also permitted by the design procedure. In order to match the imput or output impedance line of the filter to the following components, inhomogenous transformers (Fig. 1(q) and (r)) may be taken into account. The synthesis and optimization procedure will be handled in detail in another publication.

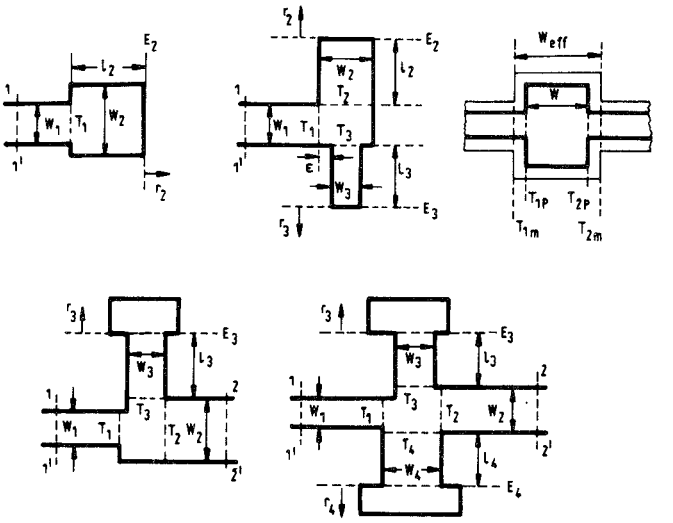

Fig. 2. Microstrip filter elements.

II. Analysis of the Filters

For the computation of microstrip filters, the corresponding geometrical structure is subdivided into individual filter elements and single discontinuity elements. The scattering matrix of these elements operated as two-ports are calculated considering conductor and dielectric loss, dispersion effects, and parasitic inductive and capacitive effects in the discontinuities. To calculate the S-matrix of the whole filter structure, the individual scattering matrices are converted into the corresponding cascade matrices, and after multiplication the resulted cascade matrix is converted into an overall scattering matrix.

The basis of the calculation procedure presented in this paper is a waveguide model representing the microstrip line [4]. It consists of two electrically conducting walls at the top and the bottom of the line and magnetic side walls (Fig. 1(a)). The effective width of the waveguide model as well as the effective dielectric constant of the medium filling the waveguide have been assumed to be frequency dependent [5], [6]. Thereby, the frequency dependence of the phase constant of the equivalent microstrip line is optimally approximated. Using this model the most important discontinuities, as those which are shown in Fig. 1, have already been calculated [6]–[12]. The comparison of the obtained theoretical results with the associated measurements shows the following.

1) The parasitic effects caused by higher order modes when calculating the dominant mode scattering matrix of microstrip discontinuities can be efficiently described by the waveguide model.

2) Due to the fast convergence of the applied method of analysis, the computation time needed to determine the S-matrix of the structures shown in Fig. 1 (which will be important in the optimization procedure) is not too high. In detail, the computer time on a control Data Cyber 76 necessary for one frequency point amounts to $5 \cdots 100$ ms.

The filter structure is calculated considering discrete filter elements, e.g., line sections, steps, bends, transformers (Fig. 1), and such elements which consist of two or more discontinuities connecting to short- or open-circuited line sections (Fig. 2).

The line section with the length l will be described by its scattering parameters:

$$s_{11} = s_{22} = 0$$
$$s_{12} = s_{21} = \exp(-j\gamma l). \tag{1}$$

Because the reference planes (T_{m1}, T_{m2}) of the discontinuities (e.g., Fig. 2(c)) which are shifted by means of the waveguide model are translated back into the physical reference planes (T_{p1}, T_{p2}), the length l in (1) is always understood as the length of two adjacent filter elements. Taking into account the conductor and dielectric losses of the line section, the propagation constant $\gamma = \alpha + j\beta$ becomes complex where β is the phase velocity and $\alpha = \alpha_d + \alpha_c$ describes the total loss. For the consideration of the dielectric attenuation factor α_d and the ohmic attenuation factor α_c, several suitable expressions are given in the literature [13]–[15], which can be taken into account.

The discrete filter elements such as steps, bends, and impedance transformers (Fig. 1) are described by their frequency dependent scattering parameters, as they are investigated in [6]–[12].

The shunt-C-element in microstrip (Fig. 1(s)) can be calculated as a cascade connection of two steps as long as the steps are not interacting via higher order modes. This means that the higher order modes excited at the first step discontinuity must be decayed vastly at the next step discontinuity. If this is not the case, the microstrip struc-

ture must be considered as a discrete filter element, and a field matching solution of the complete discontinuity problem is necessary.

The distributed C-element as a one-port can be considered either as an open-circuited impedance step (Fig. 2(a)) or as a T-junction with two open-circuited far ends (Fig. 2(b)). In these cases the reflection coefficient of the one-port r_{11} can be calculated in dependence of the scattering parameters of the corresponding discontinuity (with reference planes T_ν) and the line dimensions using the graph method as follows.

1) In the case of an open-circuited impedance step:

$$r_{11}=s_{11}^{S}+\frac{(s_{12}^{S}\cdot EX_2)^2\cdot r_2}{1-s_{22}^{W}\cdot EX_2\cdot r_2} \tag{2}$$

with $EX_\nu=\exp(-j\gamma_\nu\cdot l_\nu)$.

2) In the case of an open-circuited T-junction:

$$r_{11}=s_{11}^{T}+s_{13}^{T}\cdot EX_3\cdot A_{13}+s_{12}^{T}\cdot EX_2\cdot A_{23}$$

with

$$A_{11}=\frac{1}{r_3}-s_{33}^{T}\cdot EX_3^2; \qquad A_{22}=\frac{1}{r_2}-s_{22}^{T}\cdot EX_2^2$$

$$A_{12}=-s_{23}^{T}\cdot EX_2\cdot EX_3; \qquad NB=A_{12}^2-A_{11}A_{22}$$

$$A_{23}=(A_{12}\cdot s_{13}^{T}\cdot EX_3-A_{11}\cdot s_{12}^{T}\cdot EX_2)/NB$$

$$A_{13}=(A_{12}\cdot s_{12}^{T}\cdot EX_2-A_{22}\cdot s_{13}^{T}\cdot EX_3)/NB \tag{3}$$

where $s_{\nu\mu}^{S}$ and $s_{\nu\mu}^{T}$ are the scattering parameters of the impedance step or T-junction with the reference planes T_ν, respectively. γ_ν are the propagation constants of the lines with the width w_ν. It yields $r_2=r_3=1$ if the described structure is open-circuited in the planes E_2 or E_3 (Fig. 2(a) and (b)).

The formulas in (2) and (3) are valid as long as no higher order modes can be propagated in the considered model discontinuities. If this is not the case, the discontinuity structure must be considered as a discrete element, and a field matching solution of the discontinuity problem is necessary.

The filter element shown in Fig. 2(d) can be treated, as it is mentioned above, as a T-junction with a short-circuited, open-circuited, or mismatched far end. Using the theory of the linear networks and reciprocity theorem, the following expressions for the frequency dependent scattering parameters $s_{\nu\mu}$ of this filter element (as a two-port (Fig. 2(d))) can be obtained:

$$s_{11}=s_{11}^{T}+(s_{13}^{T}\cdot EX_3)^2/NA$$
$$s_{22}=s_{22}^{T}+(s_{23}^{T}\cdot EX_3)^2/NA$$
$$s_{12}=s_{21}=s_{12}^{T}+s_{13}^{T}\cdot s_{23}^{T}\cdot EX_3^2/NA \tag{4}$$

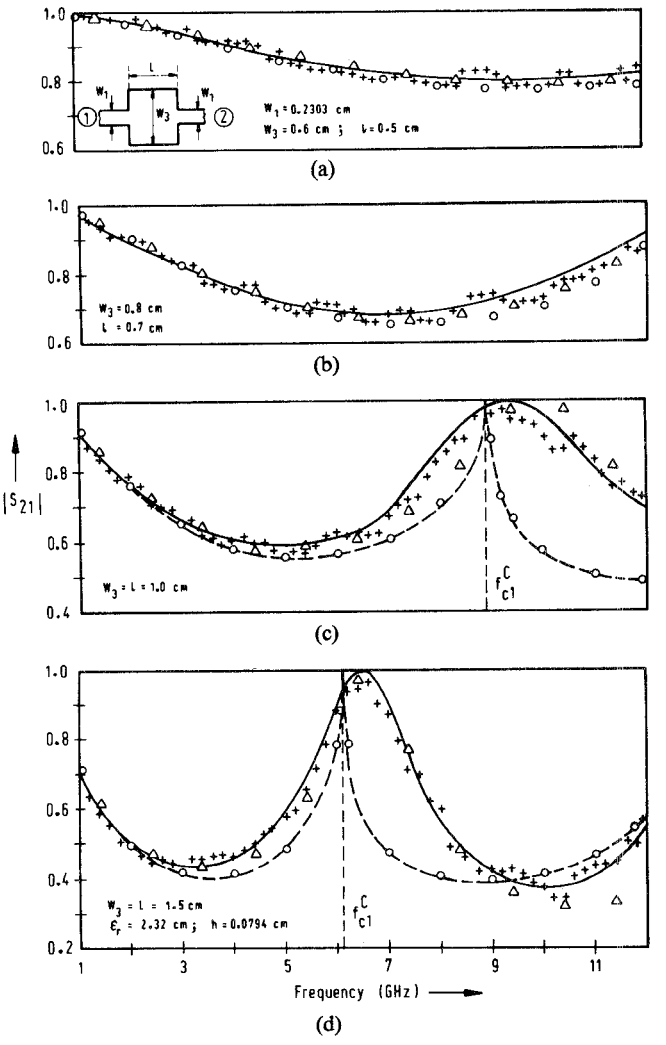

Fig. 3. Comparison between the theoretical and experimental results for the transmission coefficient $|s_{21}|$ of the distributed C-element: ——— calculated as a discrete discontinuity, △△△ calculated as a cascade connection of the impedance step-line section-impedance step, ○○○ calculated as an open-circuited crossing, and + + + + experimental points.

with $NA=1/r_3-s_{33}^{T}\cdot EX_3^2$:

$$r_3=\begin{cases}1, & \text{for open circuit in the plane } E_3\\ -1, & \text{for short circuit in the plane } E_3\\ r_{11}, & \text{for mismatched far end in the plane } E_3.\end{cases}$$

Similary, the filter element shown in Fig. 2(e) can be considered as a crossing with two open-circuited, short-circuited, or mismatched far ends. The frequency dependent scattering parameters of this filter element as a two-port are given as

$$s_{11}=s_{11}^{C}+A_{13}\cdot A_3+A_{14}\cdot A_4$$
$$s_{22}=s_{22}^{C}+A_{23}\cdot B_3+A_{24}\cdot B_4$$
$$s_{21}=s_{12}=s_{12}^{C}+A_{23}\cdot A_3+A_{24}\cdot A_4 \tag{5}$$

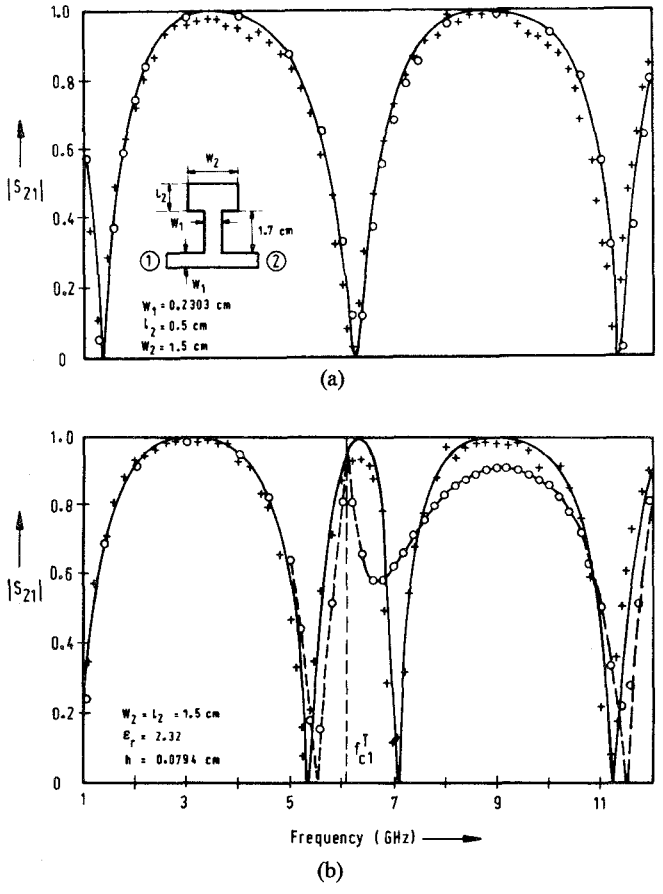

Fig. 4. Comparison between the theoretical and experimental results for the transmission coefficient $|s_{21}|$. The distributed C-element at the far end is calculated as an open-circuited impedance step (———) or as an open-circuited T-junction (○-○-○): + + + + experimental points.

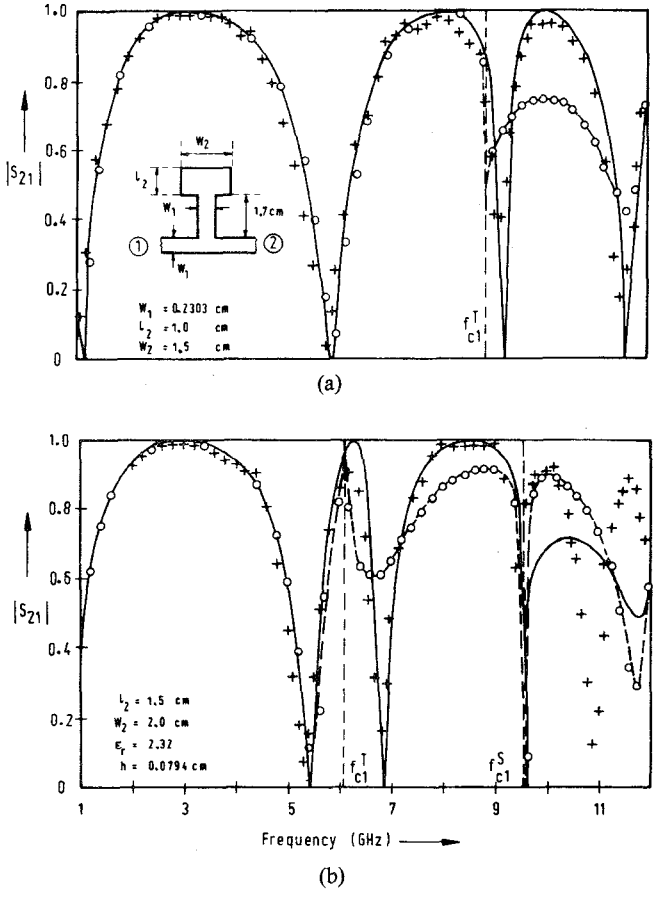

Fig. 5. Comparison between the theoretical and experimental results for the transmission coefficient $|s_{21}|$. The distributed C-element at the far end is calculated as an open-circuited impedance step (———) or as an open-circuited T-junction (○-○-○): + + + + experimental points.

with

$$A_{11}=\frac{1}{r_3}-s_{33}^{C}\cdot EX_3^2; \qquad A_{22}=\frac{1}{r_4}-s_{44}^{C}\cdot EX_4^2$$

$$A_{12}=-s_{34}^{C}\cdot EX_3\cdot EX_4; \qquad A_{13}=s_{13}^{C}\cdot EX_3$$

$$A_{23}=s_{23}^{C}\cdot EX_3; \qquad A_{14}=s_{14}^{C}\cdot EX_4$$

$$A_{24}=s_{24}^{C}\cdot EX_4; \qquad NC=A_{11}\cdot A_{22}-A_{12}^2$$

$$A_3=(A_{22}\cdot A_{13}-A_{12}\cdot A_{14})/NC;$$

$$A_4=(A_{11}\cdot A_{14}-A_{13}\cdot A_{12})/NC$$

$$B_3=(A_{22}\cdot A_{23}-A_{12}\cdot A_{24})/NC;$$

$$B_4=(A_{11}\cdot A_{24}-A_{23}\cdot A_{12})/NC$$

$$r_3=r_4=\begin{cases}1, & \text{for open circuit in the planes } E_3 \text{ and } E_4\\ -1, & \text{for short circuit in the planes } E_3 \text{ and } E_4\\ r_{11}, & \text{for mismatched far ends in the planes } E_3 \text{ and } E_4\end{cases}$$

where $s_{\nu\mu}^{C}$ are the scattering parameters of the crossing with the reference planes T_ν.

While the parasitic effects in the discontinuities are considered by means of a field-matching solution using the microstrip waveguide model, the end effects of the open-circuited line sections in the filter structure and the capacitive fringing effects in the step discontinuity must be considered using a suitable approach. Some results are reported in the available literature, e.g., [16]–[18] to calculate the end effects. In this study the end effects as well as the capacitive fringing effects in the step discontinuity are taken into account using the formulas given in [18].

III. Results

As it is mentioned above, the shunt-C-element in microstrip can be calculated as a cascade connection of two steps or as a discrete filter element. In Fig. 3 for different values of w_1 and w_3, the modulus of the transmission coefficient $|s_{21}|$ of this filter element is plotted against frequency. As it can be seen, the theoretical results of the field matching solution are in good agreement with measurements. The discrepancies between these theoretical results and those of a cascade connection treatment (for large w_3 and 1) are due to the fact that the capacitive effects in the step discontinuity are not considered correctly enough by means of the applied formulas [18]. As

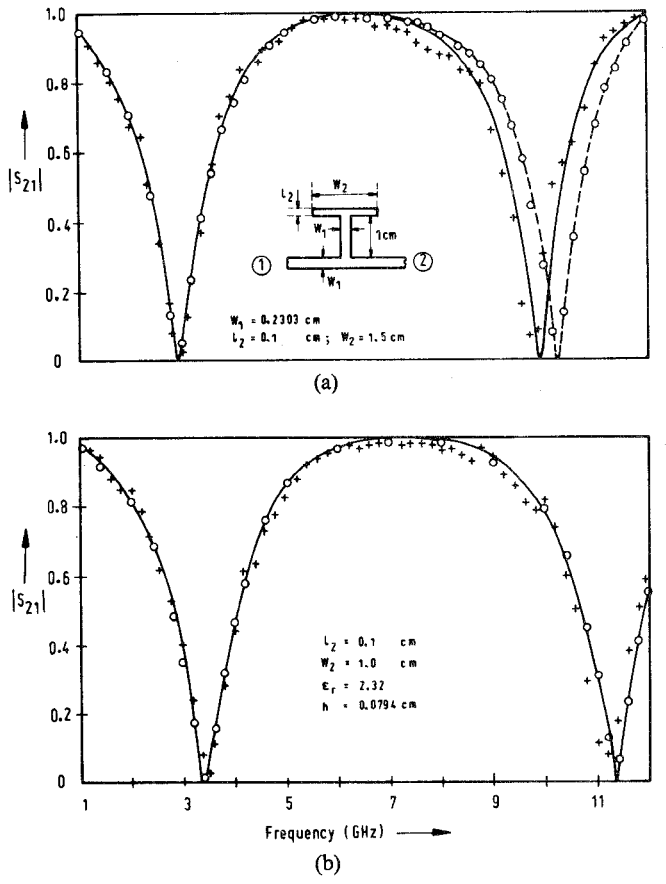

Fig. 6. Comparison between the theoretical and experimental results for the transmission coefficient $|s_{21}|$. The distributed C-element at the far end is calculated as an open-circuited impedance step (———) or as an open-circuited T-junction (OOO): ++++ experimental points.

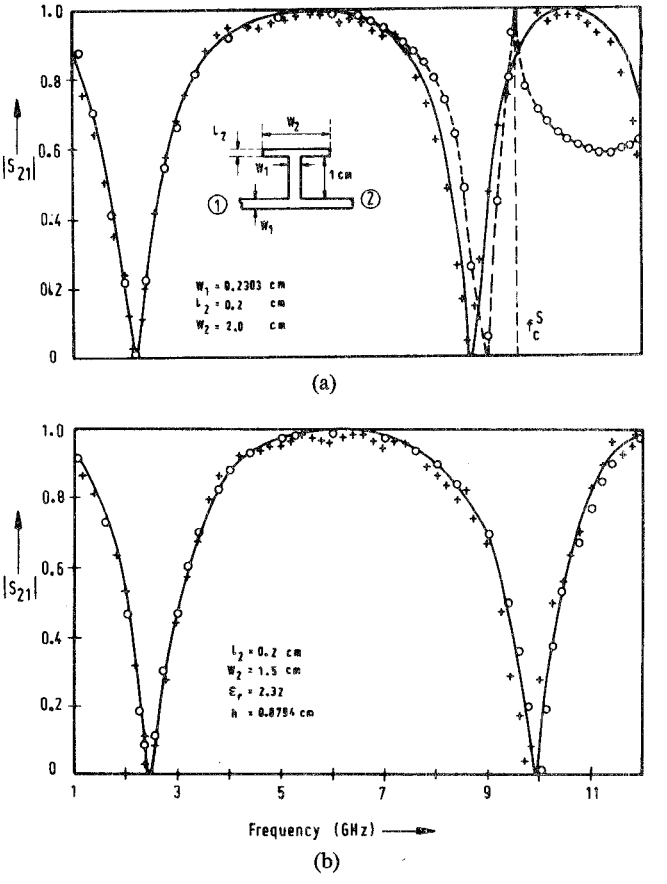

Fig. 7. Comparison between the theoretical and experimental results for the transmission coefficient $|s_{21}|$. The distributed C-element at the far end is calculated as an open-circuited impedance step (———) or as an open-circuited T-junction (OOO): ++++ experimental points.

shown in Fig. 3, the shunt-C-element can be computed as a crossing with two open-circuited ends as long as the frequency f is much smaller than the cutoff frequency f_{c1}^C of the first higher order mode in the model crossing.

Figs. 4–7 show theoretical and experimental results for a T-junction loaded with different distributed C-elements. In this the reflection coefficient r_{11} of the distributed C-element is calculated either as an open-circuited impedance step or as a T-junction with two open-circuited far ends. As seen from Figs. 4(a), 6(b), and 7(b), in both cases good agreement between theory and experiment is found if the frequency f is smaller than the cutoff frequency f_{c1}^S or f_{c1}^T of the first higher order mode in the model discontinuity [5], [6]. In this way the reflection coefficient r_{11} of the one-port can be calculated suitably as an open-circuited impedance step or as a T-junction with two open-circuited ends if $w_2 \ll l_2$ or $w_2 \gg l_2$, respectively. If the widths w_2 and 1 are too large, which means $f > f_{c1}^S$ and $f > f_{c1}^T$ (Figs. 5, 7(a)), the discontinuity problem must be computed as a discrete element using the field matching solution.

Figs. 8–10 show theoretical and experimental results for some prototype microstrip filters such as a bandpass (Fig. 8(a)), low-pass (Figs. 8(b), 9(a), and 10), and band-stop (Fig. 9(b)). In order to verify the applicability of the applied waveguide model in general the modulus of the transmission coefficient is plotted as a function of frequency f, and initially the conducting losses are not considered in the computation. Because of the strong frequency dependence of the scattering parameters, the substrate material polyguide ($\epsilon_r = 2.31$, $h = 0.156$ cm) is selected.

In order to demonstrate the good agreement between theory and experiment in Fig. 10, the modulus of transmission coefficient $|s_{21}|$ of a low-pass filter is plotted against f in an extended frequency range up to 12 GHz. The discrepancies between theory and measurement for $f > 8$ GHz are due to the radiation effects, which are of pronounced influence (as mentioned in other publications, e.g., [6]–[10]) if the substrate material polyguide ($\epsilon_r = 2.32$, $h = 0.156$ cm) is used.

IV. Conclusion

A computer-aided design procedure for microstrip filters involving junctions and discontinuities has been presented. In detail, the analysis procedure is described considering dispersion, loss, and the frequency dependent properties of microstrip discontinuities. Suitable expres-

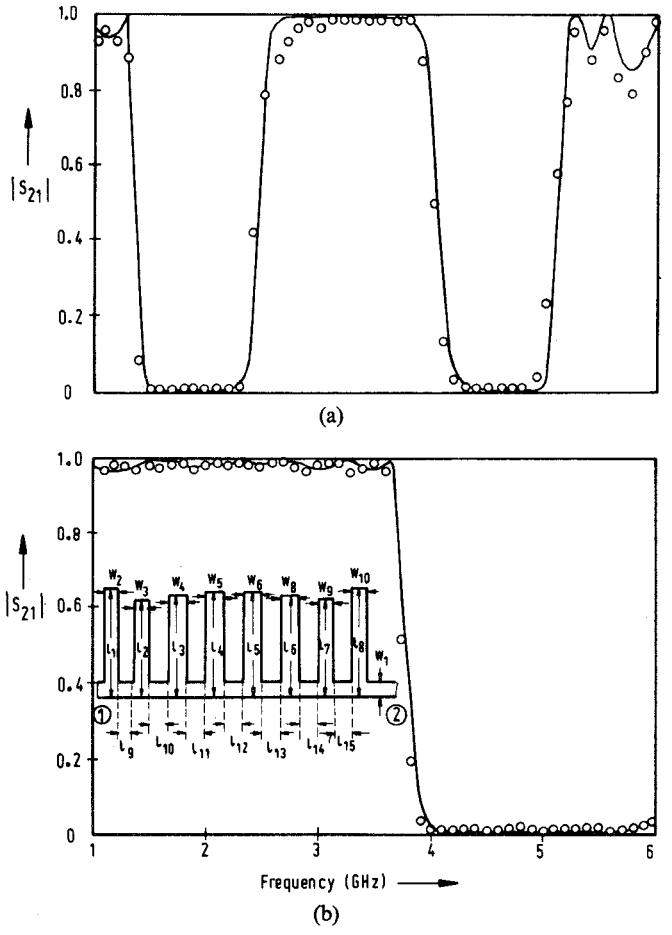

Fig. 8. Comparison between the theoretical and experimental results for the transmission coefficient $|s_{21}|$ ($\epsilon_r=2.32$, $h=0.156$ cm). (a) Butterworth bandpass filter: $W_1=0.463$ cm, $W_2=0.075$ cm, $W_3=0.46$ cm, $W_4=0.811$ cm, $W_5=0.998$ cm, $W_6=0.975$ cm, $W_8=0.805$ cm, $W_9=0.465$ cm, $W_{10}=0.075$ cm, $l_1=3.907$ cm, $l_2=3.696$ cm, $l_3=3.711$ cm, $l_4=3.774$ cm, $l_5=3.774$ cm, $l_6=3.711$ cm, $l_7=3.696$ cm, $l_8=3.907$ cm, $l_9=1.413$ cm, $l_{10}=1.071$ cm, $l_{11}=0.839$ cm, $l_{12}=0.783$ cm, $l_{13}=0.84$ cm, $l_{14}=1.08$ cm, $l_{15}=1.395$ cm. (b) Chebyshev low-pass filter: $W_1=0.467$ cm, $W_2=0.465$ cm, $W_3=0.467$ cm, $W_4=0.464$ cm, $W_5=0.466$ cm, $W_6=0.464$ cm, $W_8=0.468$ cm, $W_9=0.462$ cm, $W_{10}=0.461$ cm, $l_1=1.105$ cm, $l_2=1.395$ cm, $l_3=1.466$ cm, $l_4=1.474$ cm, $l_5=1.475$ cm, $l_6=1.463$ cm, $l_7=1.386$ cm, $l_8=1.093$ cm, $l_9=1.05$ cm, $l_{10}=1.047$ cm, $l_{11}=1.052$ cm, $l_{12}=1.047$ cm, $l_{13}=1.052$ cm, $l_{14}=1.047$ cm, $l_{15}=1.055$ cm.

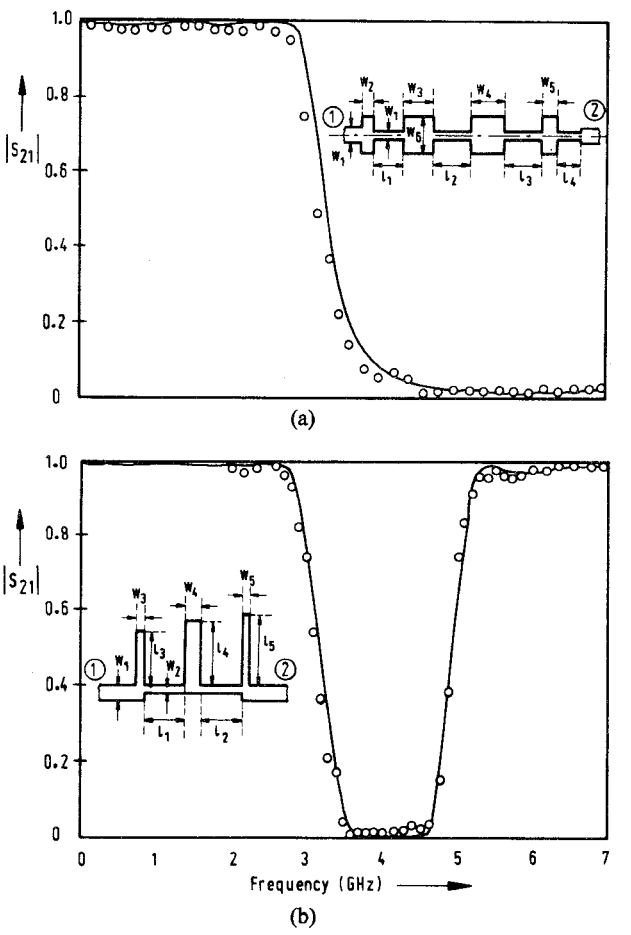

Fig. 9. Comparison between the theoretical and experimental results for the transmission coefficient $|s_{21}|$ ($\epsilon_r=2.32$, $h=0.156$ cm). (a) Chebyshev low-pass filter: $W_1=0.476$ cm, $W_2=0.325$ cm, $W_3=0.815$ cm, $W_4=0.83$ cm, $W_5=0.665$ cm, $W_6=0.094$ cm, $l_1=0.925$ cm, $l_2=1.095$ cm, $l_3=1.075$ cm, $l_4=0.57$ cm. (b) Band-stop filter: $W_1=0.230$ cm, $W_2=1.1$ cm, $W_3=W_5=0.3$ cm, $W_4=0.12$ cm, $l_1=1.33$ cm, $l_2=1.3$ cm, $l_3=1.287$ cm, $l_4=1.375$ cm, $l_5=1.49$ cm.

sions for calculating filter elements in microstrip which consist of two or more discontinuities connected to short- or open-circuited line sections are given. It is shown that the analysis procedure using a waveguide model turns out to be an efficient tool for practical filter design technique giving high accuracy and fast numerical computation. The theoretical results for several examples of prototype microstrip filter structures are compared with measurements. It is found that the analysis procedure leads to results which are strongly supported by measurements. The computer time (central processing time on a CD Cyber 76) required for the calculation of the scattering matrix of the investigated filter structures at one frequency point amounts to 50$\cdots$120 ms.

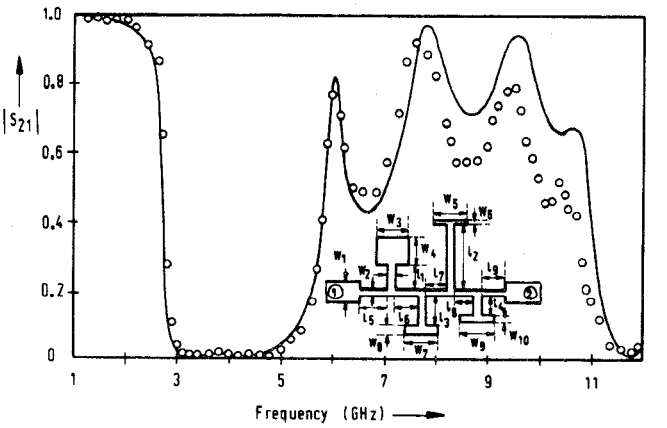

Fig. 10. Comparison between the theoretical and experimental results for the transmission coefficient $|s_{21}|$ of a low-pass filter ($\epsilon_r=2.32$, $h=0.156$ cm): $W_1=0.476$ cm, $W_2=0.047$ cm, $W_3=0.79$ cm, $W_4=0.489$ cm, $W_5=0.284$ cm, $W_6=0.364$ cm, $W_7=0.4$ cm, $W_8=0.437$ cm, $W_9=0.4$ cm, $W_{10}=0.437$ cm, $l_1=0.35$ cm, $l_2=1.01$ cm, $l_3=0.767$ cm, $l_4=0.767$ cm, $l_5=0.585$ cm, $l_6=0.689$ cm, $l_7=0.52$ cm, $l_8=0.58$ cm, $l_9=0.42$ cm.

ACKNOWLEDGMENT

The numerical calculations have been done at the computing center of the University of Duisburg. Thanks are due to Prof. Dr.-Ing. I. Wolff who encouraged this work.

REFERENCES

[1] G. L. Mathei, L. Young, and F. M. T. Jones, *Microwave Filters, Impedance-Matching Networks and Coupling Structures*. New York: McGraw-Hill, 1964.
[2] R. Levy, "Tables of element values for the distributed low-pass prototype filter," *IEEE Trans. Microwave Theory Tech.*, vol. MTT-13, pp. 514–535, Sept. 1965.
[3] G. C. Temes and S. K. Mitra, *Modern Filter Theory and Design*. New York: Wiley, 1973.
[4] I. Wolff, G. Kompa, and R. Mehran, "Calculation method for microstrip discontinuities and T-junctions," *Electron. Lett.*, vol. 8, pp. 177–179, Apr. 1972.
[5] G. Kompa and R. Mehran, "Planar waveguide model for calculating microstrip components," *Electron. Lett.*, vol. 11, pp. 459–460, Sept. 1975.
[6] R. Mehran, "The frequency-dependent scattering matrix of microstrip right-angle bends, T-junctions and crossings," *Arch. Elek. Ubertragung*, vol. 29, pp. 454–460, Nov. 1975.
[7] G. Kompa, "S-matrix computation of microstrip discontinuities with a planar waveguide model," *Arch. Elek. Ubertragung*, vol. 30, pp. 58–64, Feb. 1976.
[8] W. Menzel and I. Wolff, "A method for calculating the frequency dependent properties of microstrip discontinuities," *IEEE Trans. Microwave Theory Tech.*, vol. MTT-25, pp. 107–112, Feb. 1977.
[9] R. Mehran, "The frequency-dependent scattering matrix of twofold truncated microstrip bends," *Arch. Elek. Ubertragung*, vol. 31, pp. 411–415, Oct. 1977.
[10] ——, "Calculation of microstrip bends and Y-junctions with arbitrary angle," *IEEE Trans. Microwave Theory Tech.*, vol. MTT-26, June 1978.
[11] W. Menzel, "Calculation of inhomogenous microstrip lines," *Electron. Lett.*, vol. 13, pp. 183–184, Mar. 1977.
[12] G. Kompa, "Design of stepped microstrip components," *Radio Electron. Eng.*, vol. 48, pp. 53–63, Jan./Feb. 1978.
[13] R. A. Pucel, D. J. Massé, and C. P. Hartwig, "Losses in microstrip," *IEEE Trans. Microwave Theory Tech.*, vol. MTT-16, pp. 342–350, June 1968.
[14] I. J. Bahl and R. Garg, "A designer's guide to stripline circuits," *Microwaves*, pp. 90–95, Jan. 1978.
[15] R. H. Jansen, "High-speed computation of single and coupled microstrip parameters including dispersion, high-order modes, loss and finite strip thickness," *IEEE Trans. Microwave Theory Tech.*, vol. MTT-26, Feb. 1978.
[16] L. Lewin, "Radiation from discontinuities in strip line," *Proc. Inst. Elec. Eng.*, vol. 107, part C, pp. 163–170, Feb. 1960.
[17] P. Silvester and P. Benedek, "Equivalent capacitance of microstrip open circuits," *IEEE Trans. Microwave Theory Tech.*, vol. MTT-20, pp. 511–516, 1972.
[18] E. O. Hammerstad, "Equations for microstrip circuit design," in *Proc. 5th European Microwave Conf.* Sevenoaks, Kent, England: Microwave Exhibitions and Publishers, Ltd., 1975, pp. 268–272.

The Low-Noise 115-GHz Receiver on the Columbia-GISS 4-ft Radio Telescope

HONG-IH CONG, ANTHONY R. KERR, SENIOR MEMBER, IEEE, AND ROBERT J. MATTAUCH, MEMBER, IEEE

Abstract—**The superheterodyne millimeter-wave radiometer on the Columbia-GISS 4-ft telescope is described. This receiver uses a room-temperature Schottky diode mixer, with a resonant-ring filter as LO diplexer. The diplexer has low signal loss, efficient LO power coupling, and suppresses most of the LO noise at both sidebands. The receiver IF section has a parametric amplifier as its first stage with sufficient gain to overcome the second-stage amplifier noise. A broad-banded quarter-wave impedance transformer minimizes the mismatch between mixer and paramp. At 115 GHz, the SSB receiver noise temperature is 860 K, which is believed to be the lowest figure so far reported for a room-temperature receiver at this frequency.**

Manuscript received June 26, 1978; revised September 28, 1978.

H. I. Cong and A. R. Kerr are with NASA Goddard Institute for Space Studies, Goddard Space Flight Center, New York, NY 10025.
R. J. Mattauch is with the Department of Electrical Engineering, University of Virginia, Charlottesville, VA 22901.

I. INTRODUCTION

THE COLUMBIA-GISS 4-ft radio telescope was constructed for the purpose of surveying the distribution of carbon monoxide in the interstellar space of our Galaxy. The telescope, a Cassegrain with an effective f/D ratio of 2.8, has a half-power beamwidth of 8 arc min at 115 GHz, the frequency of the fundamental rotational transition line of carbon monoxide. The receiver front-end is of the superheterodyne type using a room-temperature Schottky diode mixer, followed by a 1.39-GHz parametric amplifier with a noise temperature of 50 K and a gain of ~17 dB. At 115 GHz, the single-sideband noise temperature of this receiver is 860 K, which we believe to be the best performance reported at this frequency for a room-

0018-9480/79/0300-0245$00.75 ©1979 IEEE